Thalamic Hypometabolism in mTBI: Insight from Data Driven Voxelwise Analysis of 3D 1H-MR Spectroscopy Imaging

Xiaodan YAN[1], Ivan Kirov[1], and Oded Gonen[1]
[1]*Radiology, New York University, New York, NY, United States*

Introduction

Traumatic brain injury (TBI) and related disabilities affect nearly 5.3 million people in the U.S, imposing a costly economic burden of about $56 billion. Diagnosis based on the Glassgow Coma Scale (GCS) indicates that 85% of TBI cases are mild (GCS:13-15). Mild-TBI (mTBI) pathology was previously believed to be "microscopic" and "diffuse" diseases. ^{1}H MR spectroscopy imaging (MRSI) is a noninvasive technique for detecting microscopic and metabolic changes in the brain. In order to investigate whether there are focal metabolic changes associated with mTBI, a data-driven voxelwise analysis was adapted after MRSI data was co-registered to a standard space. This rigorous statistical approach avoids the bias and errors from manually outlining regions of interest (ROI-s).

Methods & Results

Twenty-six mTBI patients and 13 age-matched controls were recruited, with GCS score 15-13 and confirmed loss of consciousness for less than 30 minutes. MRI and MRSI were acquired on 3 T Simenens Trio scanner with a TEM3000 circularly-polarized, transmit-receive head-coil. 160 1-mm thick slices of Magnetization Prepared RApid Gradient Echo (MP-RAGE): TE/TI/TR= 2.6/800/1360 ms, was obtained with FOV=256×256 mm^2 and 512×512 matrix. Our chemical-shift imaging (CSI) based auto-shim procedure then adjusted the scanner's first and second order currents in 3-5 minutes [1]. Next, a 10 cm anterior-posterior (AP) ×8 cm left-right (LR) ×4.5 cm inferior-superior (IS) = 360 cm^3 VOI was image-guided over the corpus callosum (Fig.1). VOI was excited with *TE*/*TR*=35/1800 ms PRESS in three second-order Hadamard encoded slabs (6 slices) interleaved every *TR* along the IS direction for optimal signal-to-noise ratio (SNR) and spatial coverage [2]. The six slices were partitioned with 2D 16×16 CSI over a 16×16 cm^2 (LR×AP) FOV, to yield 1.0×1.0×0.75 cm^3 voxels. The 8×10 cm (LR×AP) VOI was defined in their planes with two 11.2 ms numerically optimized 180° pulses under 1.34 and 1.1 mT/m to yield 8×10×6=480 voxels. The MR signal was acquired for 256 ms at ±1 kHz bandwidth. The ^{1}H-MRSI data was processed offline using in-house software written in IDL. Data was voxel-shifted to align NAA grid with VOI. Then data was Fourier transformed in the time, AP and LR dimensions and Hadamard reconstructed along the IS direction. The 480 spectra were each frequency-aligned and zero-order phase corrected in reference to the NAA peak in every voxel. The relative levels of the *i*-th (*i*=NAA, Cr, Cho, *m*I, Glu) metabolite in the *j*-th (*j*=1…480) voxel and *k*-th (*k*=1...40) measurement were estimated from their peak area, S_{ijk}, using the SITools-FITT parametric spectral modeling package (using aspartate, glutamate, glutamine, Cho, Cr, *m*I, NAA and taurine functions) of Soher *et al.*[3]. Each 16×16×6 S_{ijk} matrices were then linearly interpolated to *j*=256×256×192 in order to have the same spatial resolution (V_{voxel}=1 mm^3 isotropic voxels) and FOV as the MP-RAGE images, using our in-house software. Note that although this interpolation does not add information to the data, it produces overlapping voxels that can reduce partial volume [4]. The 256×256×192 S_{ijk} matrices were then aligned by our software with their anatomical MP-RAGE MRI based on the VOI offset information. The anatomical images of each individual were registered to the Talairach space [5] after skull-stripping with AFNI (http://afni.nimh.nih.gov/). Both the S_{ijk}-s and S'_{ijk}-s were subsequently warped onto their anatomical images in standard space by applying the same transformation matrix (Fig.2). After co-registering each individual data into the standard space, an independent two-sample *t*-test was applied to investigate group differences of metabolic concentration for each metabolite on each voxel. Significant clusters were detected with combined criteria on size of cluster and individual *p*-value, which was determined from AlphaSim software in AFNI. Significant differences were shown in the thalamus for NAA, Cr, Cho and *m*I, and also at putamen for NAA and Cr (Fig.3). Average S_{ijk}-*s* were extracted from these clusters for further quantification. Firstly, S_{ijk}-*s* were divided by the CSF fraction of the corresponding voxel, then The concentration in the *m*-th ROI for the *i*-th metabolite in the *k*-th measurement, C_{ikm}, was obtained relative to a 2 L sphere of Ci^{vitro}=12.5, 10.0, 3.0, 7.5 and 12.5 mM NAA, Cr, Cho, mI and Glu in water at physiological ionic strength to load the coil. The VOI size and position (in the coil and the magnet) were chosen to be similar to the in vivo studies in order to sample the B1 profile of the coil closely as in (1), where S_{iR} is the average signal of the *i*-th metabolite in the phantom in the same unites as S'_{ijk}, V_k180° and V_R180° are the RF voltage into 50 omega required for a non-selective 1 ms 180° inversion pulse on the k-th measurement and reference. The C_{imk}-*s* were corrected for *in vivo* ($T1_i^{vivo}$, $T2_i^{vivo}$) and *in vitro* ($T1_i^{vitro}$, $T2_i^{vitro}$) relaxation time differences (2). Quantification of metabolic concentration in thalamus and putamen are shown in Table 1 and Fig. 4. Significant group difference is found for NAA, Cr, Cho and mI in thalamus, and significant difference for Cho and NAA in right putamen, with mTBI patients showing decreased concentrations.

$$C_{ikm} = \frac{C_i^{vitro}}{S_{iR}} \cdot \frac{\sum_j S'_{ijk} \cdot M_{jm}}{\sum_j M_{jm}} \cdot \frac{V_k^{180^\circ}}{V_R^{180^\circ}} \cdot f_i \quad \text{mM} \qquad (1)$$

$$f_i = \frac{\exp\left(-TE/T_{2i}^{vitro}\right)}{\exp\left(-TE/T_{2i}^{vivo}\right)} \cdot \frac{1-\exp\left(-TR/T_{1i}^{vitro}\right)}{1-\exp\left(-TR/T_{1i}^{vivo}\right)} \qquad (2)$$

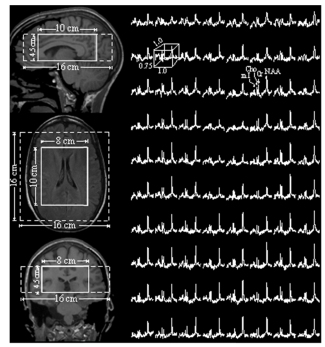

Fig.1: VOI and spectra of 3D MRSI.

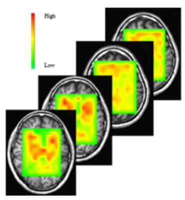

Fig.2 Co-registration of MRI and MRSI.

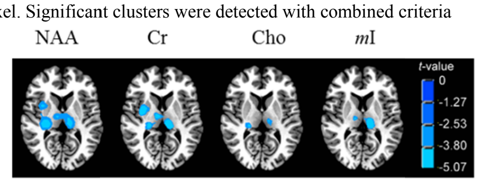

Fig.3: Regions showing significant difference from voxelwise t-test (TBI-Ctrl). Radiology orientation was adapted (viewer's right of the left of the brain).

			NAA	Cr	Cho	mI
Thalamus	L	TBI	7.86+1.85	6.20+1.41	1.47+0.34	6.47+1.22
		Ctrl	9.22+1.34	7.12+1.04	1.62+0.30	7.29+1.20
	R	TBI	7.83+1.49	6.10+1.08	1.53+0.29	6.21+0.90
		Ctrl	9.00+0.96	6.91+0.89	1.61+0.20	6.81+0.98
Putamen	L	TBI	7.07+2.17	5.69+1.80	1.11+0.35	6.53+1.65
		Ctrl	7.22+1.98	5.78+1.66	1.06+0.31	6.61+1.85
	R	TBI	6.90+1.40	6.11+1.01	1.23+0.31	5.70+1.19
		Ctrl	7.58+1.15	6.75+1.08	1.28+0.24	6.53+1.07

Table 1: Quantification of metabolic concentration at thalamus and putamen.

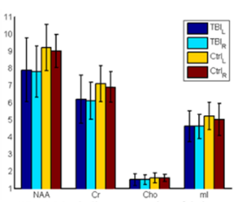

Fig.4: Metabolic concentration of thalamus.

Discussion & Conclusion

The present study, with data-driven voxelwise analysis of 3D ^{1}H MRSI, found decreased metabolic concentration of NAA, Cr, Cho and *m*I at thalamus and putamen. This is consistent with a few previous reports on thalamic dysfunction among mTBI, such as hypoactivation from fMRI study [6][7], decreased regional cerebral blood flow [8], which was correlated with neurocognitive functioning [8]. Furthermore, deep brain stimulation on the thalamus led to behavioral improvement in a severe TBI patient [9]. A recent study also found decreased thickness in thalamus and putamen [10]. The present study together with previous relevant studies, indicate hypometabolism of thalamus (and parts of putamen) may contribute to mTBI pathology.

Reference

[1] Hu J, Javaid T, Arias-Mendoza F, Liu Z, McNamara R, Brown TR. A fast, reliable, automatic shimming procedure using 1H chemical-shift-imaging spectroscopy. J Magn Reson B 1995; 108:213-219.
[2] Goelman G, Liu S, Hess D, Gonen O. Optimizing the efficiency of high-field multivoxel spectroscopic imaging by multiplexing in space and time. Magn Reson Med 2006; 56:34-40.
[3] Soher BJ, Young K, Govindaraju V, Maudsley AA. Automated spectral analysis III: application to in vivo proton MR spectroscopy and spectroscopic imaging. Magn Reson Med 1998; 40: 822-831.
[4] Bernstein MA, Fain SB, Riederer SJ. Effect of windowing and zero-filled reconstruction of MRI data on spatial resolution and acquisition strategy. J Magn Reson Imaging; 2001: 14, 270-280.
[5] Talairach, J., Tournoux, P., 1988. Co-planar stereotaxic atlas of the human brain: 3-dimensional proportional system: an approach to cerebral imaging. Thieme.
[6] Mayer AR, Mannell MV, Ling J, Elgie R, Gasparovic C, Phillips JP, Doezema D, and Ronald AY. Auditory Orienting and Inhibition of Return in Mild Traumatic, Brain Injury: A FMRI study. 2009; 30:4152-4166.
[7] Gosselin N, Bottari C, Chen JK, Petrides M, Tinawi S, Guise E, Ptito A. Electrophysiology and Functional MRI in Post-Acute Mild Traumatic Brain Injury. 2011; 28: 329-341.
[8] Ge Y, Patel MB, Chen Q, Grossman EJ, Zhang K, Miles L, Babb JS, Reaume J, Grossman RI. Assessment of thalamic perfusion in patients with mild traumatic brain injury by true FISP arterial spin labelling MR imaging at 3T. Brain Inj, 2009, 23:666-674.
[9] Schiff ND, Giacino JT, Kalmar K, Victor JD, Baker K, Gerber M, Fritz B, Eisenberg B, O'Connor J, Kobylarz EJ, Farris S, Machado A, McCagg C, Plum F, Fins JJ & Rezai AR. Behavioural improvements with thalamic stimulation after severe traumatic brain injury. 2008. Nature. 2007;448:600-3.
[10] Zhou Y, Tang L, Sodickson DK, Reaume J, Grossman RI, Ge Y. MRI Morphological and Functional Connectivity Analysis of Thalamus in Mild Traumatic Brain Injury. 2011, Proc. Intl. Soc. Mag. Reson. Med. 19.